Electronic Supplementary Information

Nanoparticle-assembled interconnected $PbO_{1.44}$ hollowspheres enabled by PVP-driven transformation of β-PbO_2 and self-sacrificial templating for superior lithium storage

Xiaoxu Bo,*‡[a] Jiatong Zhang,‡[b] Qian Zhang,[b] Ruijie Wu,[b] Sheng Wang,[a] Shiqiang Zhao*[b] and Shun Wang*[b]

[a.] Department of Agriculture and Biotechnology, Wenzhou Vocational College of Science and Technology, Wenzhou 325006, P. R. China.

[b.] Key Lab of Advanced Energy Storage and Conversion of Wenzhou, Key Lab of Carbon Materials of Zhejiang Province, College of Chemistry and Materials Engineering, Wenzhou University, Wenzhou 325035, P. R. China.

‡These authors contributed equally to this work.

*Corresponding author:

[a.] E-mail: boxxsci@163.com (X. Bo)

[b.] E-mail: zhaosq@wzu.edu.cn (S. Zhao), shunwang@wzu.edu.cn (S. Wang)

Experimental Section

1. Materials

All chemicals are analytic grade and were used as received. Lead acetate ($Pb(Ac)_2 \cdot 3H_2O$, 99%), sodium hydroxide (NaOH, 99%) and ammonium persulfate ($(NH_4)_2S_2O_8$, 99%) were purchased from Shanghai Meryer Chemical Technology Corporation. Polyvinylpyrrolidone K30 (PVP, 99%) was purchased from Badische Anilin-und-Soda-Fabrik Corporation. Ultrapure water (18.2 MΩ·cm) was used throughout the solution preparation.

2. Material Synthesis

2.1 PVP-assisted synthesis of $PbO_{1.44}$ nanoparticle-assembled hollowspheres ($PbO_{1.44}$ NAHSs)

$PbO_{1.44}$ NAHSs were fabricated by a facile hydrothermal reaction of $Pb(Ac)_2 \cdot 3H_2O$, NaOH and $(NH_4)_2S_2O_8$ in the presence of PVP. In a typical synthesis process, $Pb(Ac)_2 \cdot 3H_2O$ (0.8 mmol) and PVP (0.12 g, 3.0 g L^{-1}) powders were ultrasonically dispersed in a 50 mL Teflon-lined autoclave containing 20 mL of water. NaOH (44 mmol) and $(NH_4)_2S_2O_8$ (2.4 mmol) powders were ultrasonically dispersed and dissolved in 10 mL of water in two beakers, respectively. Then, the NaOH and $(NH_4)_2S_2O_8$ solutions were successively added dropwise into the above 50 mL Teflon-lined autoclave containing $Pb(Ac)_2 \cdot 3H_2O$ and PVP solution under vigorous stirring. Afterwards, the Teflon-lined autoclave was sealed and kept in a thermostatic chamber at 120 °C for 7 h. Finally, the autoclave was cooled down to room temperature and the dark-brown precipitates of $PbO_{1.44}$ NAHSs were collected by centrifugation, washed with ultrapure water and anhydrous ethanol for three times each, and dried in a vacuum oven at 80 °C for 12 h.

2.2 Time and PVP concentration control experiments

To reveal the formation mechanism of $PbO_{1.44}$ NAHSs, time-dependent experiments were performed at the designed incubation times of 1, 3 and 5 h. To investigate the unique role of PVP in the formation of $PbO_{1.44}$ NAHSs, a series of PVP concentration control experiments were systematically conducted and investigated, that is, the concentrations of PVP in the 40 mL reaction solution were designed as 0, 0.5, 1.0, 1.5, 2.0 and 2.5 g L^{-1}. Therein, β-PbO_2 microspheres (MSs) were synthesized in the absence of PVP (0 g L^{-1}). The mixtures of $PbO_{1.44}$ NAHSs and β-PbO_2 MSs were obtained in the presence of PVP (0.5, 1.0, 1.5, 2.0 and 2.5 g L^{-1}), and the amount ratios of $PbO_{1.44}$ NAHSs in the mixtures were increased along with the improved PVP concentrations.

3. Characterizations

3.1 Structural Characterizations

Scanning electron microscopy (SEM) measurements were performed using a field emission source operated at an accelerating voltage of 15 kV by ZEISS sigma 500. The SEM samples were prepared by dispersing the samples of interest in ethanol via ultrasonication for 30 min, followed by deposition and

drying on a silicon substrate. Transmission electron microscopy (TEM) images, high resolution transmission electron microscopy (HRTEM) images and selected area electron diffraction (SAED) ring patterns were obtained using a transmission electron microscope instrument (TEM, JEM-2100F). Powder X-ray diffraction (XRD, Bruker AXS D8 Advance) measurements were performed using Cu-Kα radiation (40 kV, 120 mA) with a step of 4° per 25 s and a 2θ range of 10-80°. X-ray photoelectron spectroscopy (XPS) measurements were carried out on a Thermo Scientific ESCALAB 250Xi electron spectrometer using Al Kα radiation (15 kV, 10 mA). Brunauer-Emmet-Teller (BET) isotherms and specific surface areas were determined using a Micromeritics ASAP 2460 3.01 sorptometer. After the electrochemical performance tests, the cycled electrodes of the $PbO_{1.44}$ NAHSs and β-PbO_2 MSs were obtained by disassembling the cells, rinsing with dimethyl carbonate (DMC), drying at room temperature in an argon-filled glove box, and sealing in glass vials for subsequent characterizations.

3.2 Electrochemical Measurements

To make working electrodes, after dispersing the synthesized active material of $PbO_{1.44}$ NAHSs or β-PbO_2 MSs, acetylene black and sodium alginate in a weight ratio of 7:2:1 in ultrapure water, the resulting homogeneous slurry obtained after grinding was pasted onto a copper foil and dried under vacuum at 80°C for 12 h. The foil was then cut into discs (12 mm in diameter). The average loading density of active materials in the working electrodes is 2.0 ± 0.2 mg cm^{-2}. For assembling the lithium coin cells, lithium foil, polypropylene (Celgard 2500, Celgard Inc., USA) and 1 mol L^{-1} $LiPF_6$ in ethylene carbonate (EC)/dimethyl carbonate (DMC) (volume ratio, 1:1) with 5 wt.% fluoroethylene carbonate (FEC) were used as counter electrode, separator and electrolyte, respectively. The CR2032-type coin cells were assembled in an argon-filled glove box (MIKROUNA).

Galvanostatic cycling tests of $PbO_{1.44}$ NAHSs and β-PbO_2 MSs were performed using a LAND CT2001A system (Wuhan Landian) over the voltage range of 0.01-3.0 V (vs. Li^+/Li). Prior to each galvanostatic cycling test at the high current rate of 500 mA g^{-1}, the cells were first activated at 50 mA g^{-1} for three cycles. Cyclic voltammetry (CV) curves were collected on a Shanghai Chenhua electrochemical workstation at a scan rate of 0.2 mV s^{-1} over the voltage range of 0.01-3.0 V (vs. Li^+/Li). Electrochemical impedance spectroscopy (EIS) measurements were also performed on the freshly assembled cells using the Shanghai Chenhua electrochemical workstation over a frequency range of 10^{-2}-10^5 Hz by applying a perturbation of 0.005 V. For the Galvanostatic Intermittent Titration Technique (GITT) tests, the cells were discharged or charged at 50 mA g^{-1} for 30 mins, followed by an equal duration relaxation process under open circuit for 60 mins, allowing the equilibrium potential of the lithium storage at different points to be probed in the whole voltage window of 0.01-3.0 V.

Supplementary Figures

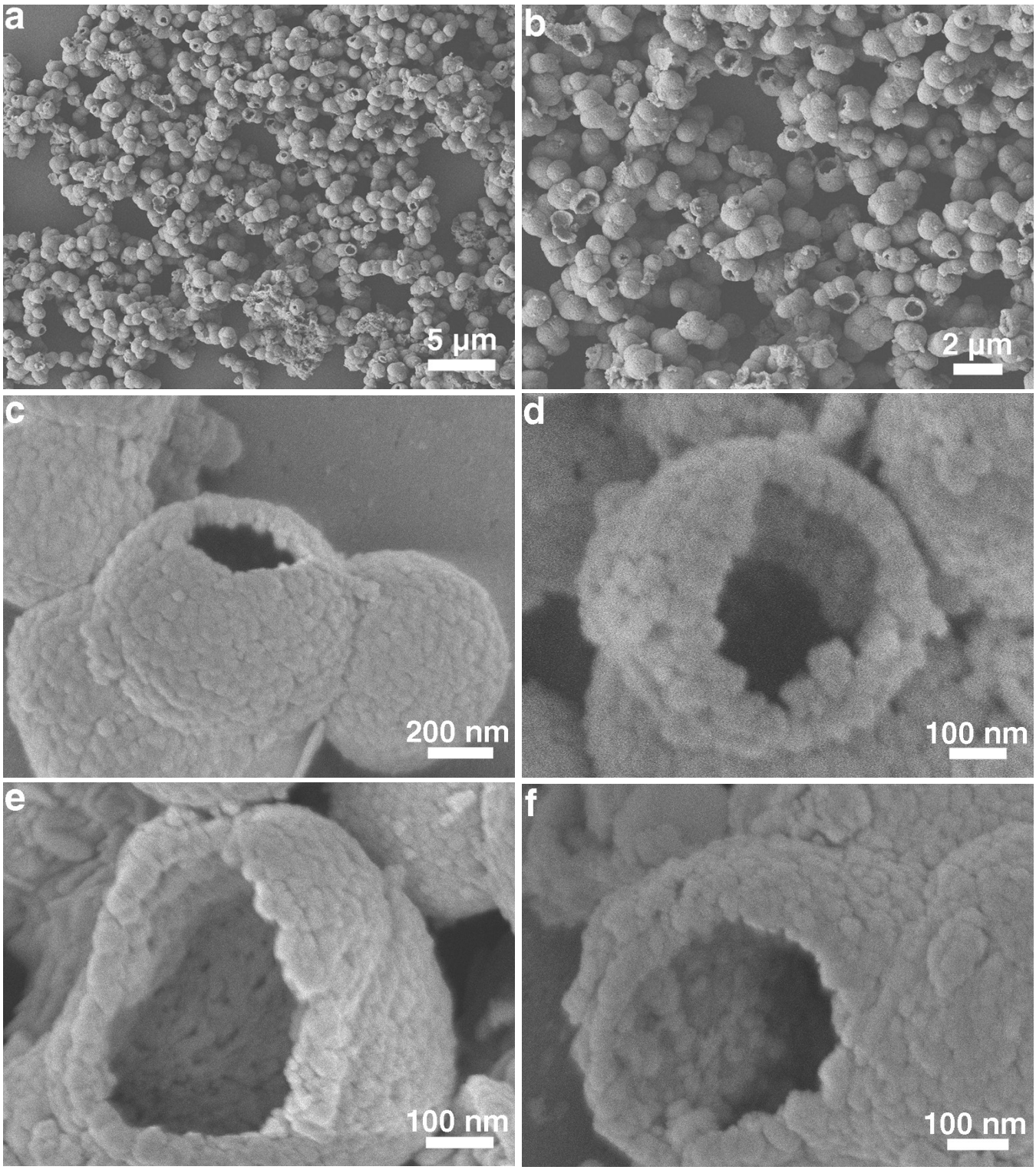

Figure S1. SEM images of $PbO_{1.44}$ NAHSs synthesized in the presence of PVP (3 g L^{-1}).

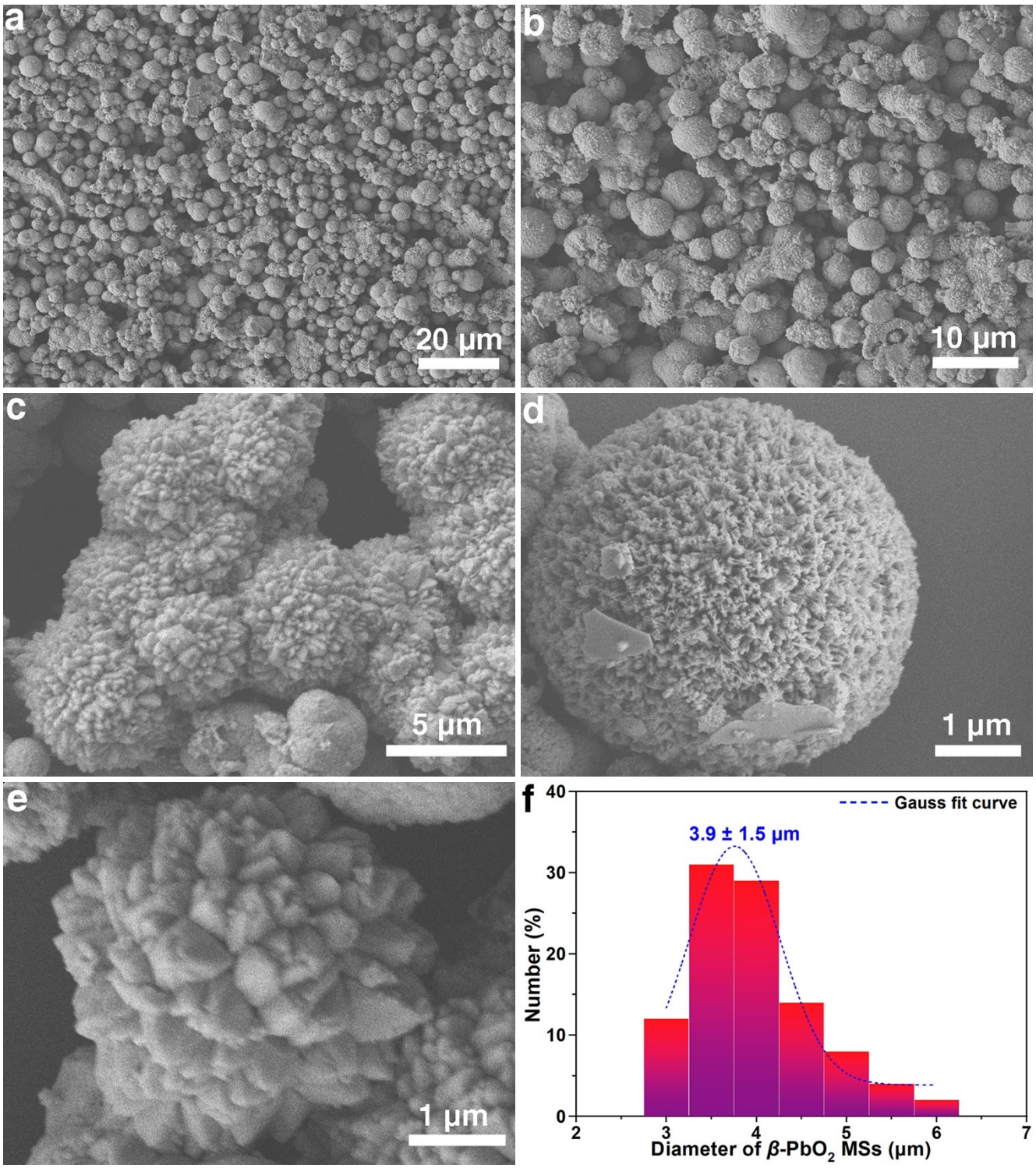

Figure S2. (a-e) SEM images and (f) diameter distribution of β-PbO_2 MSs obtained in the absence of PVP.

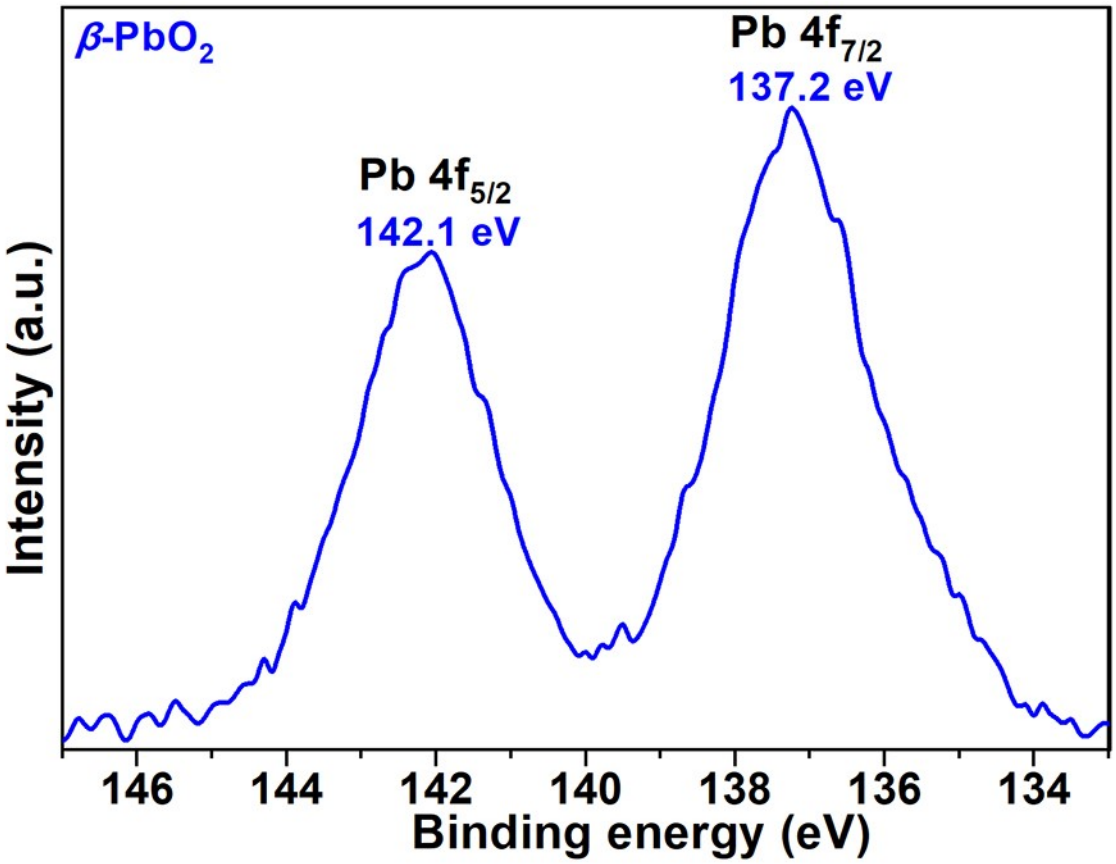

Figure S3. XPS spectrum of Pb 4f of β-PbO_2 MSs obtained in the absence of PVP.

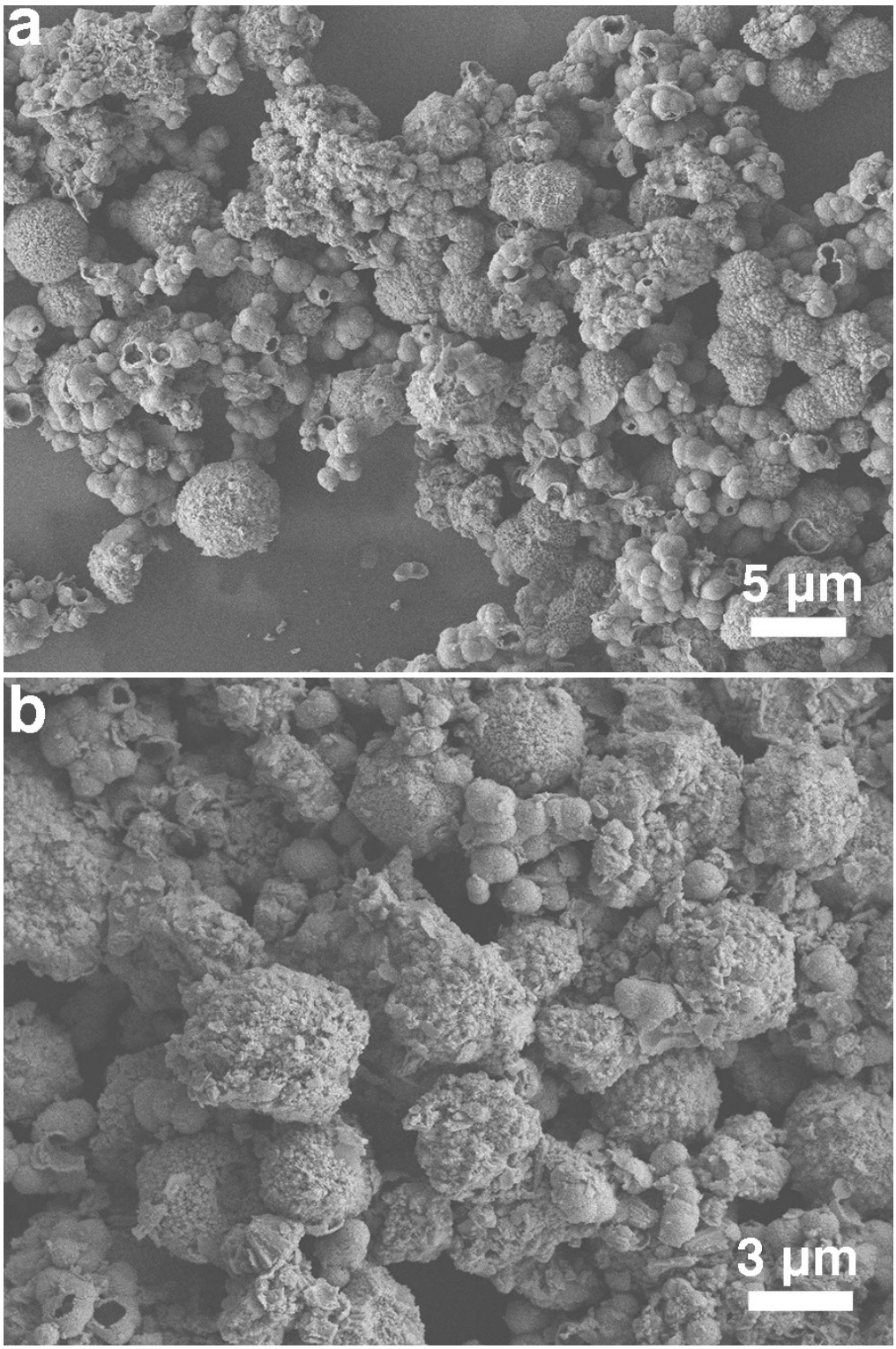

Figure S4. SEM images of the mixture of β-PbO_2 MSs (primary) and $PbO_{1.44}$ NAHSs (secondary) obtained in the presence of 0.5 g L^{-1} PVP.

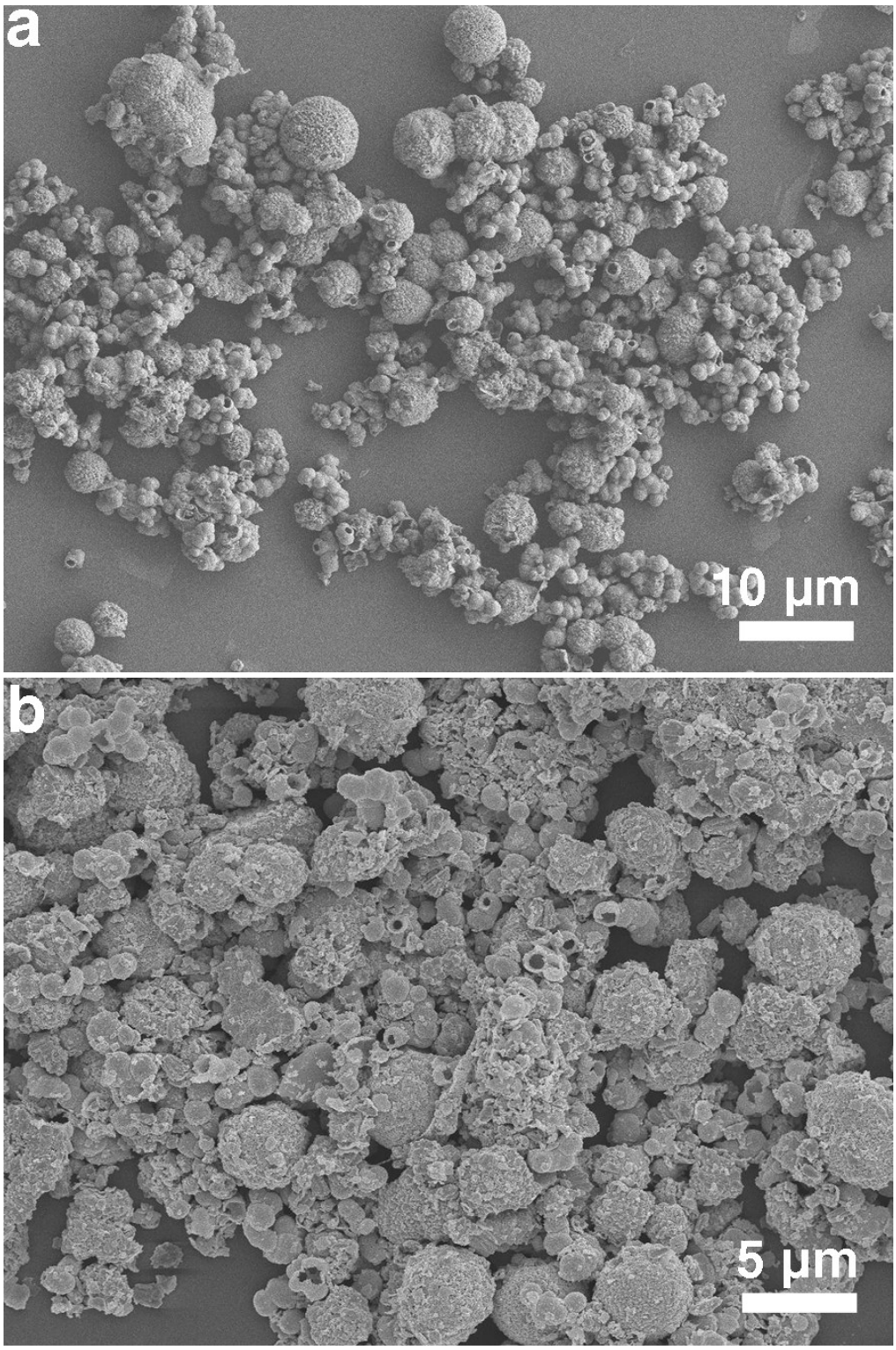

Figure S5. SEM images of the mixture of β-PbO_2 MSs (primary) and $PbO_{1.44}$ NAHSs (secondary) obtained in the presence of 1.0 g L^{-1} PVP.

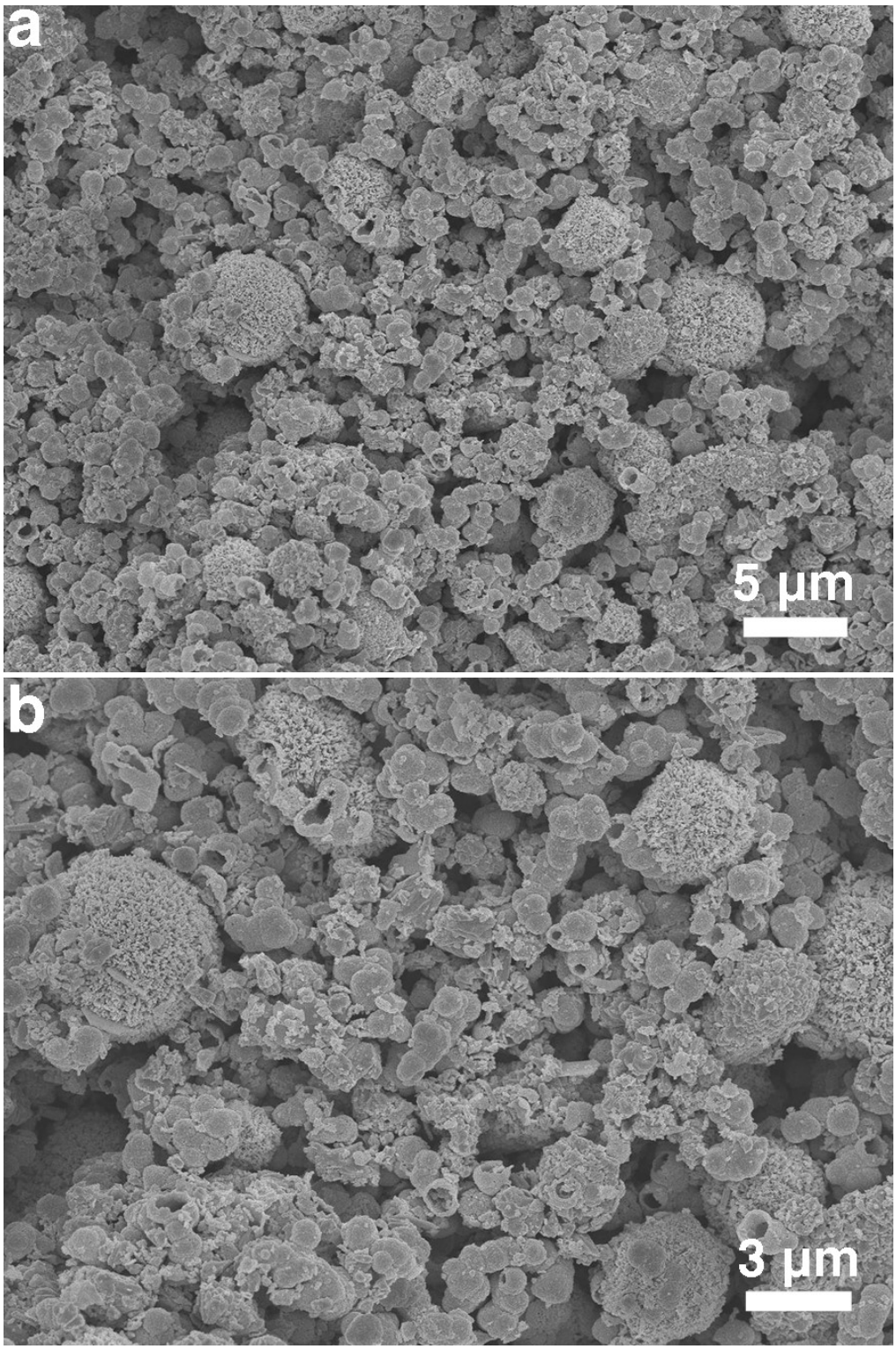

Figure S6. SEM images of the mixture of $PbO_{1.44}$ NAHSs and β-PbO_2 MSs obtained in the presence of 1.5 g L^{-1} PVP.

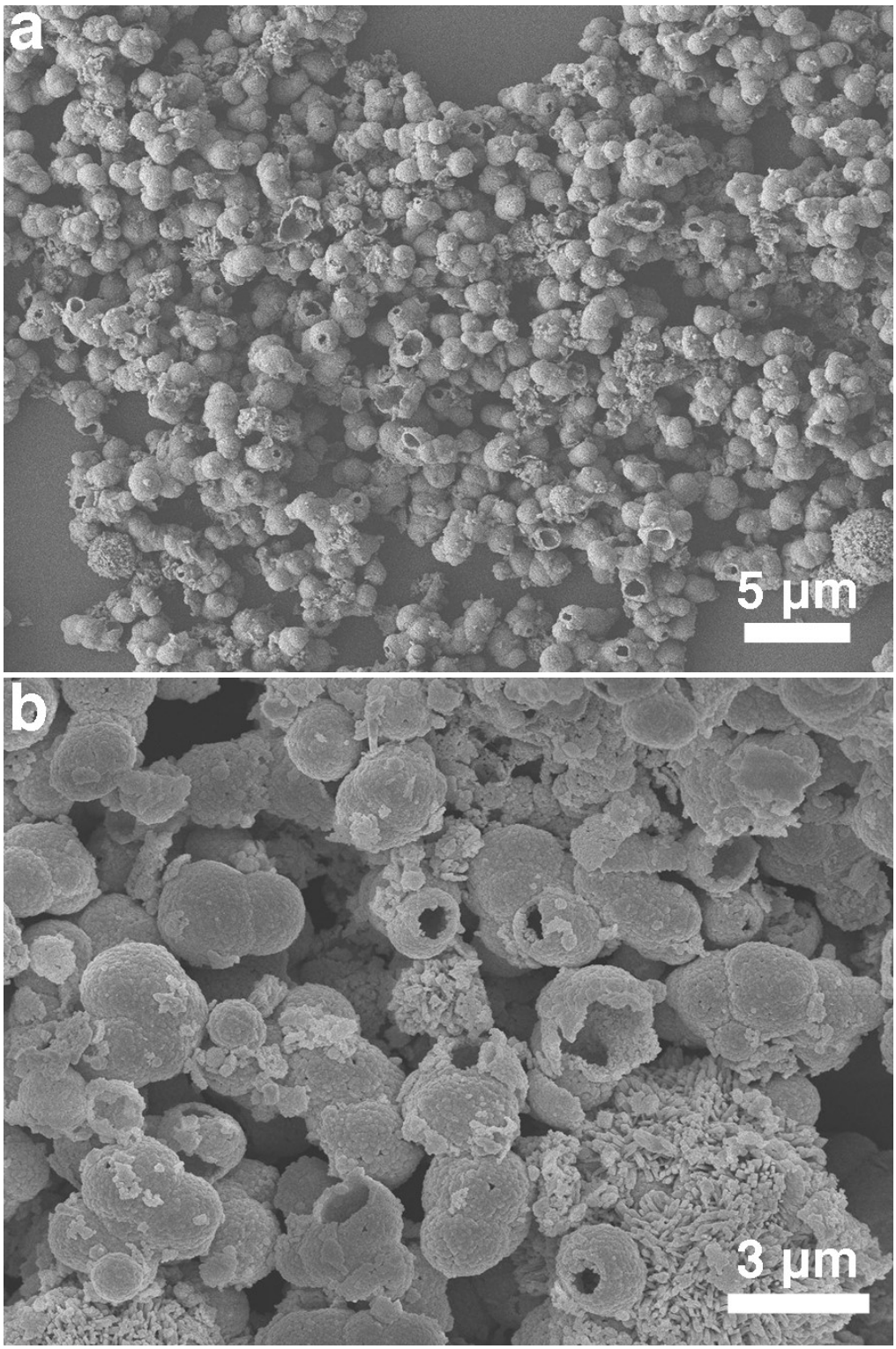

Figure S7. SEM images of the mixture of $PbO_{1.44}$ NAHSs (primary) and β-PbO_2 MSs (secondary) obtained in the presence of 2.0 g L^{-1} PVP.

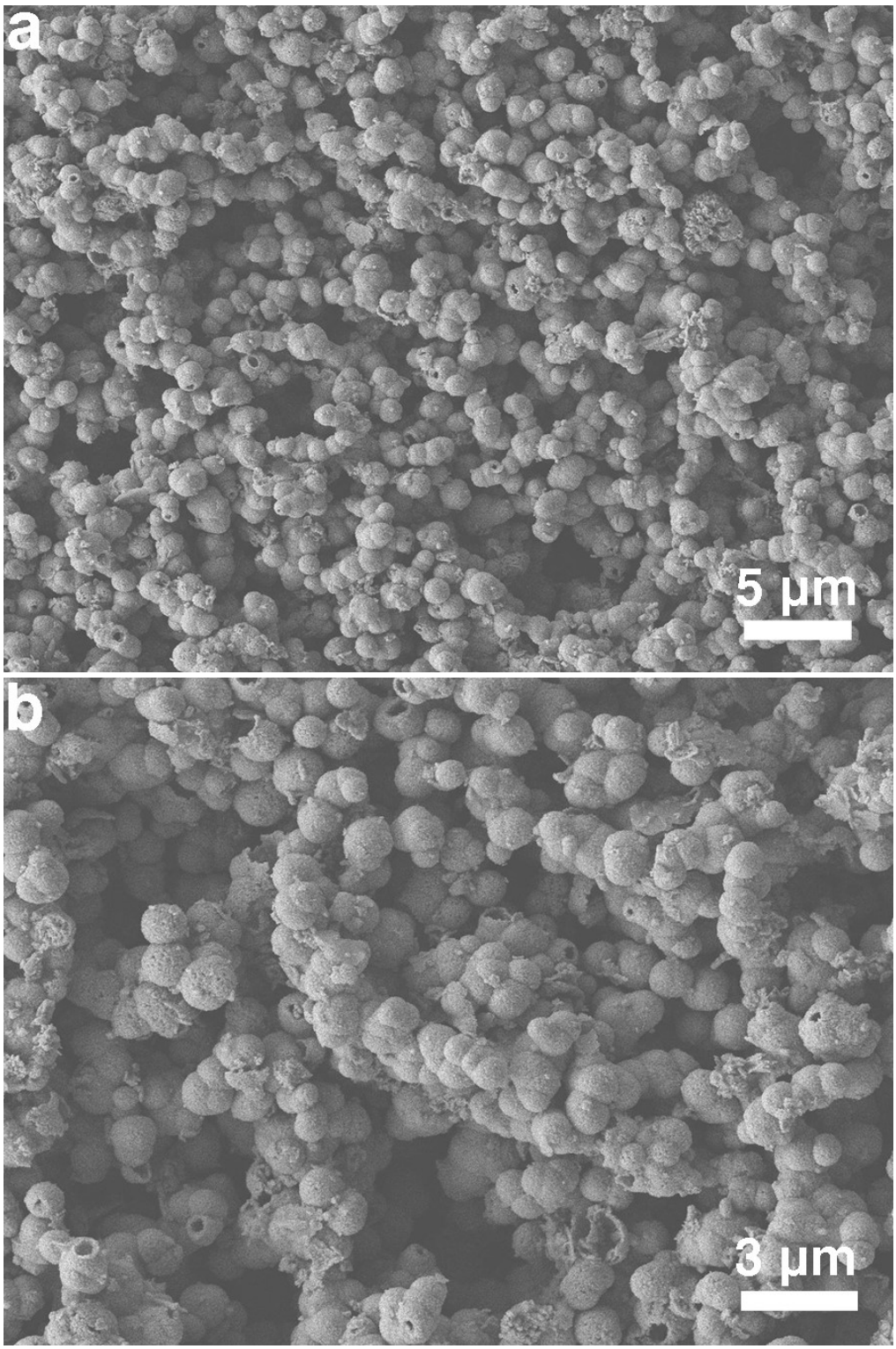

Figure S8. SEM images of the mixture of $PbO_{1.44}$ NAHSs (primary) and fragments of β-PbO_2 MSs (secondary) obtained in the presence of 2.5 g L^{-1} PVP.

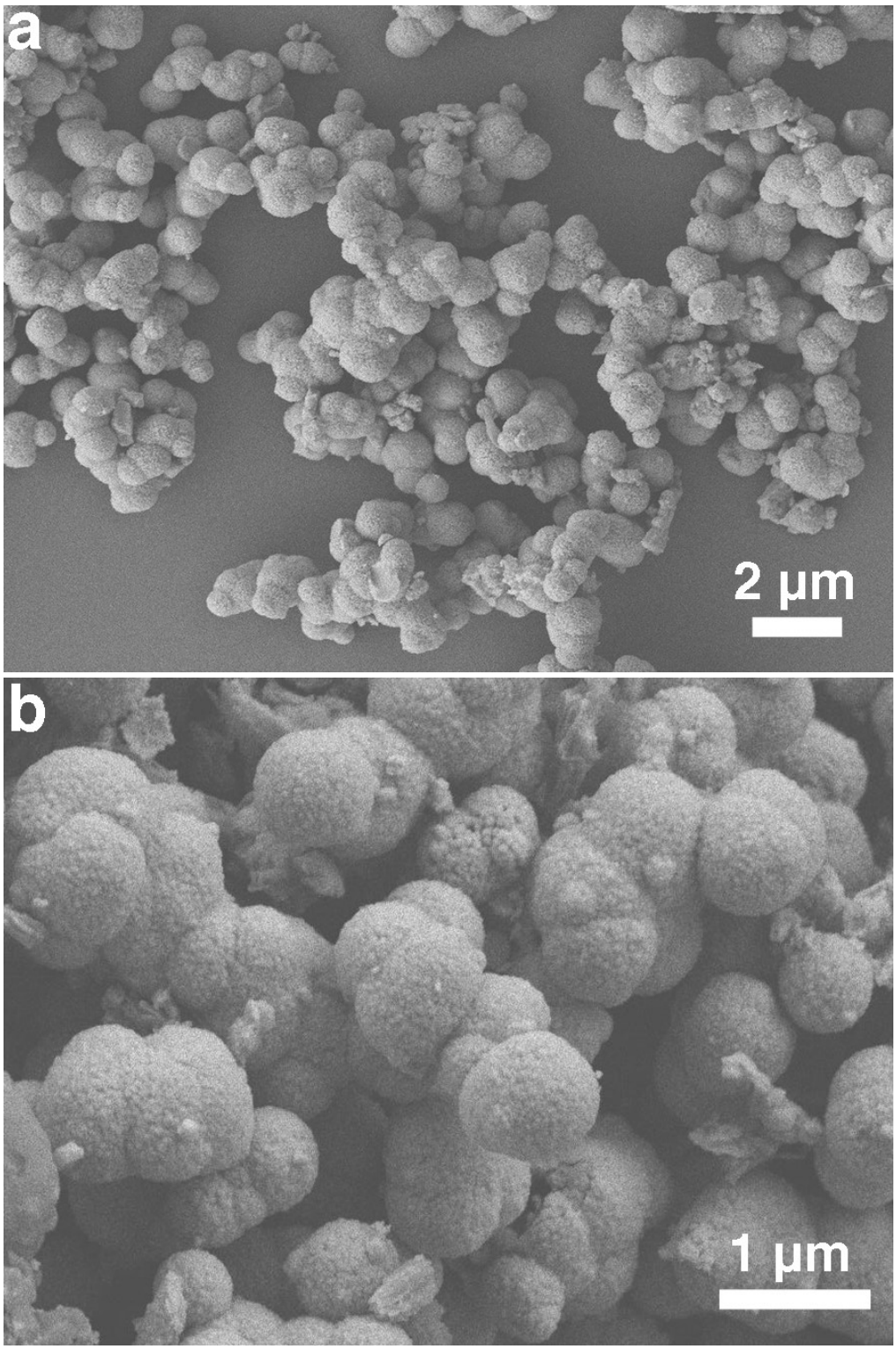

Figure S9. SEM images of the mixtures of $PbO_{1.44}$ NAHSs (primary) and β-PbO_2 MSs (secondary) obtained from the time dependent experiment at 1 h.

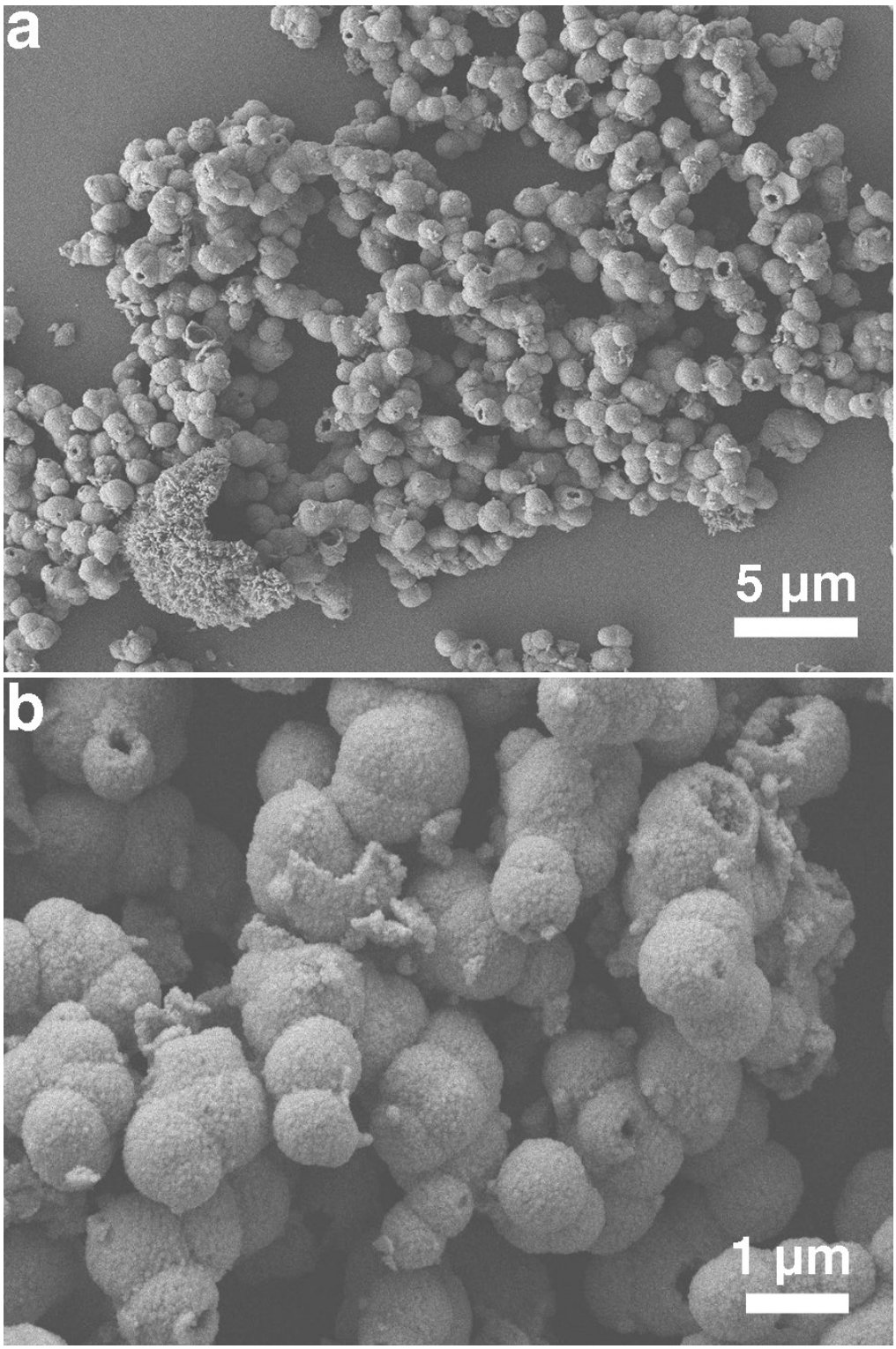

Figure S10. SEM images of the mixtures of $PbO_{1.44}$ NAHSs (primary) and β-PbO_2 MSs (secondary) obtained from the time dependent experiment at 3 h.

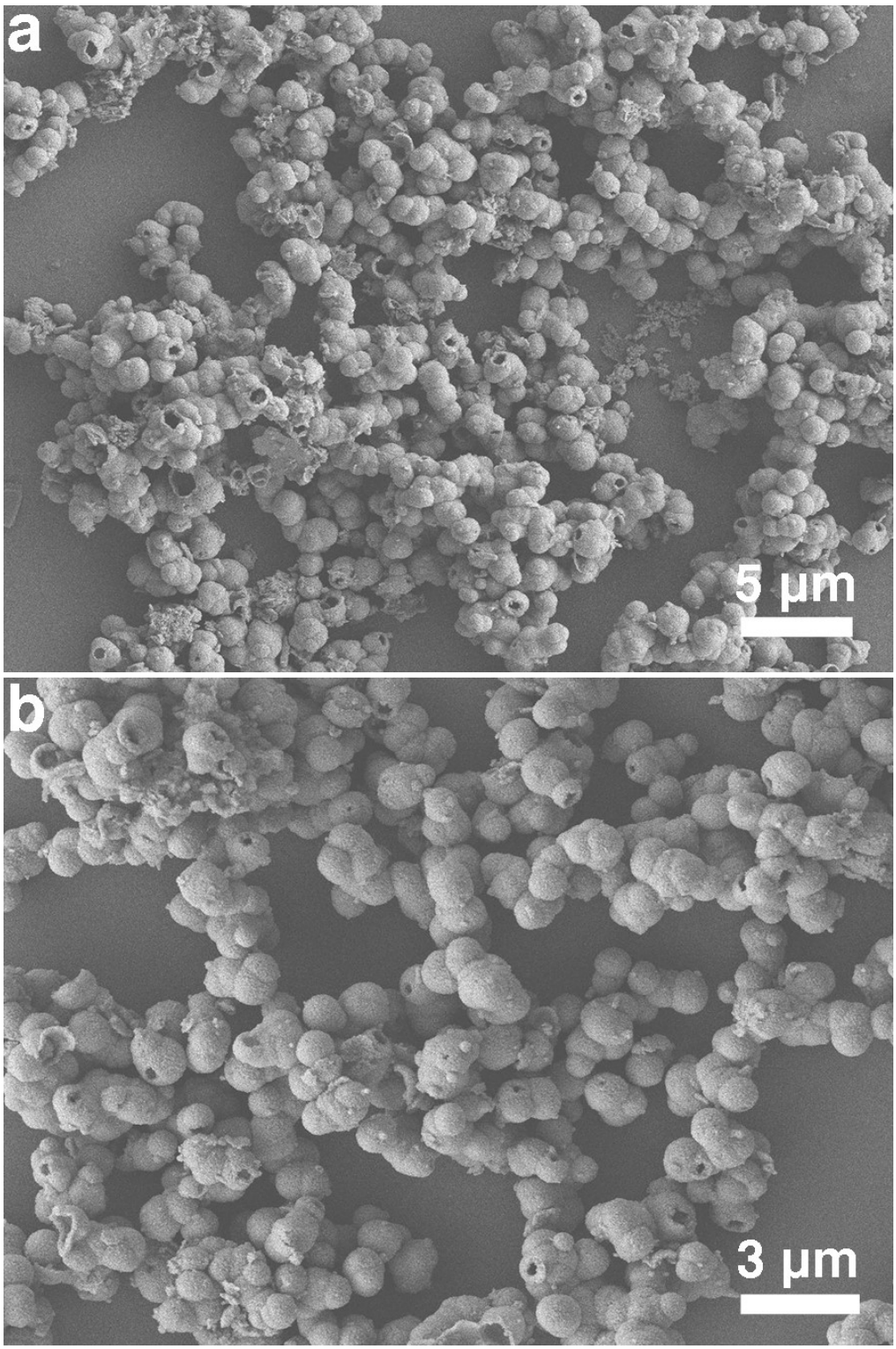

Figure S11. SEM images of the mixtures of $PbO_{1.44}$ NAHSs (primary) and fragments of β-PbO_2 MSs (secondary) obtained from the time dependent experiment at 5 h.

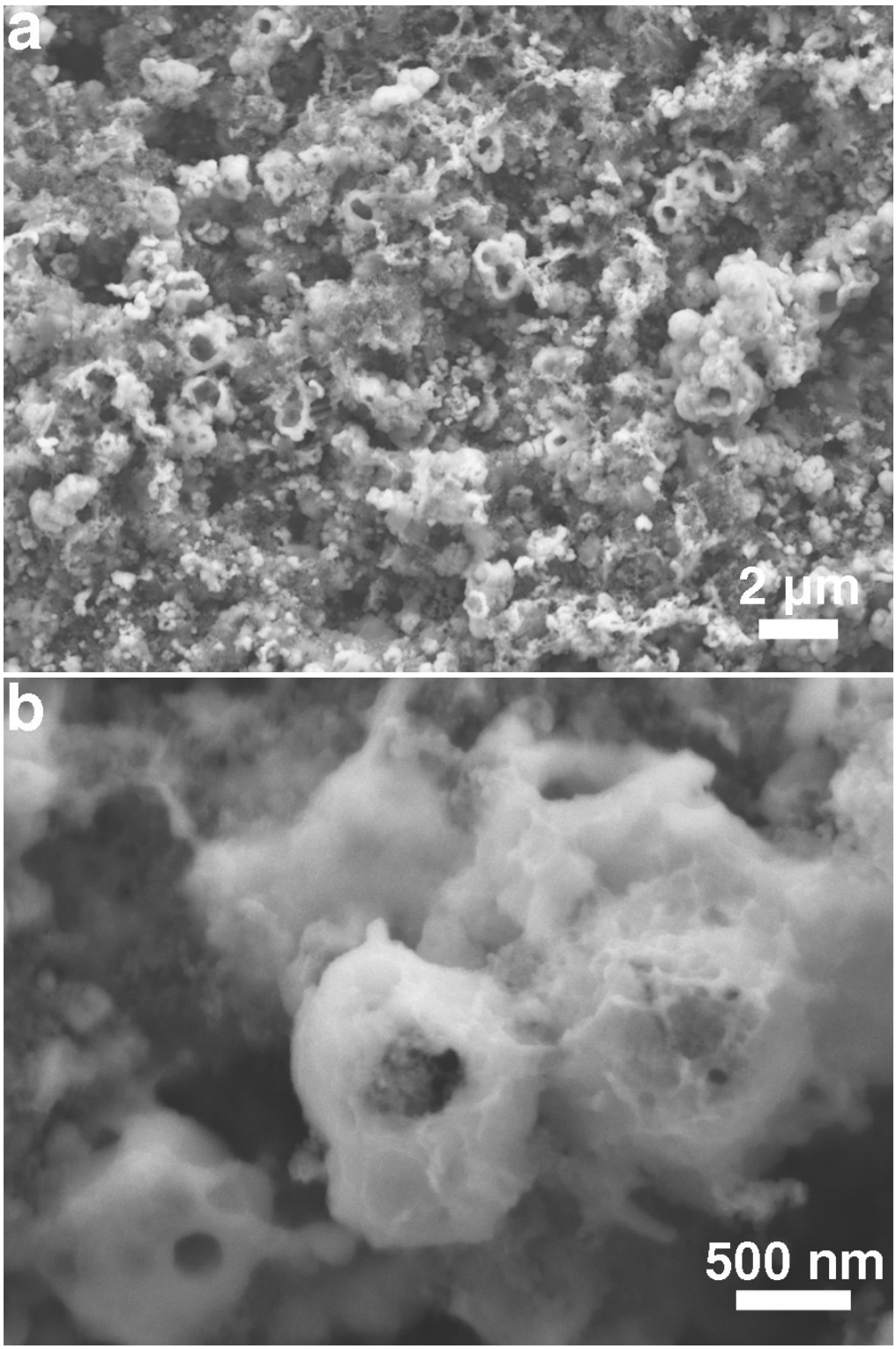

Figure S12. SEM images of the cycled electrode of $PbO_{1.44}$ NAHSs obtained after the 90th cycle in the rate performance test (Figure 5c).

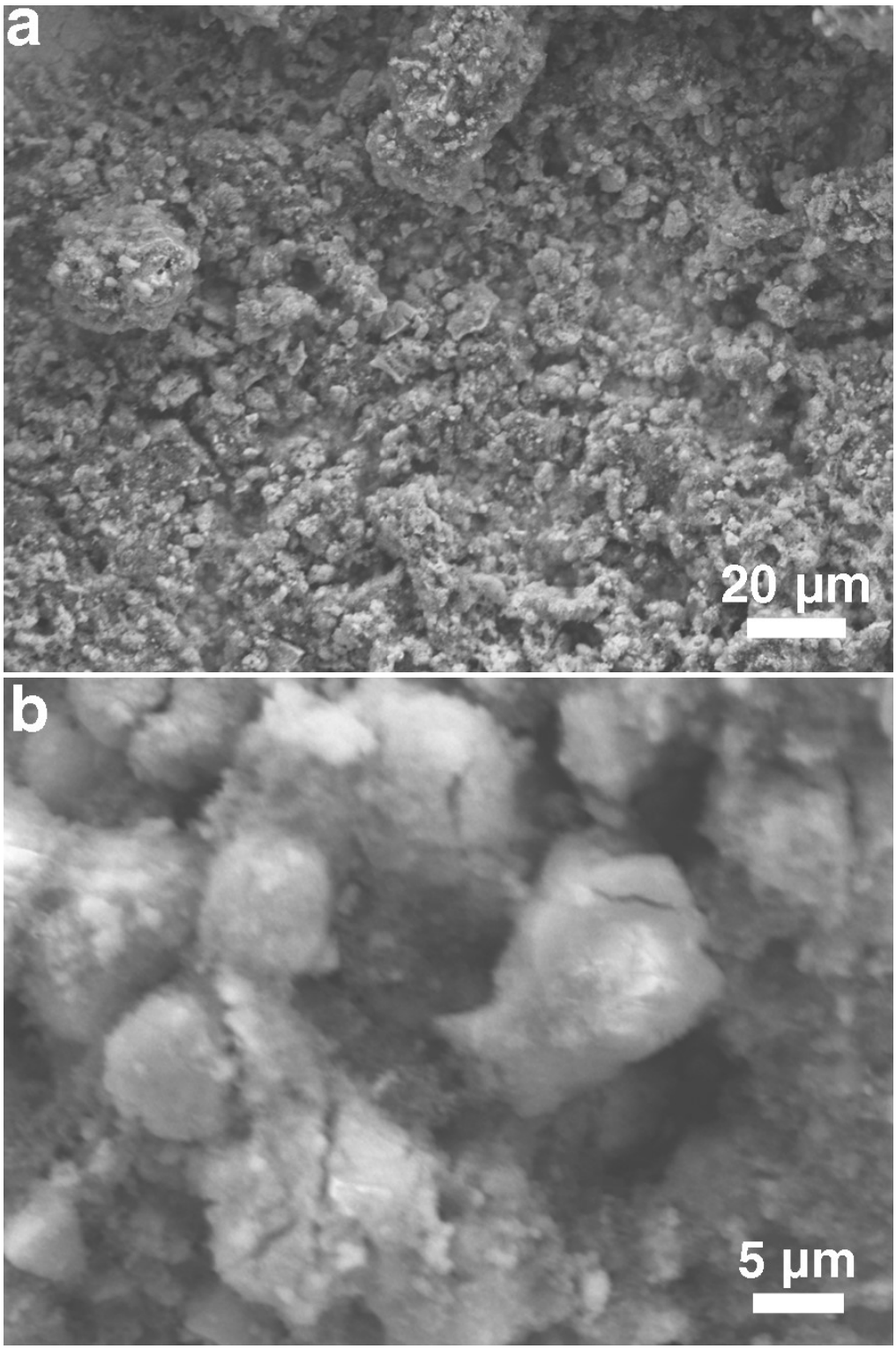

Figure S13. SEM images of the cycled electrode of β-PbO_2 MSs obtained after the 90th cycle in the rate performance test (Figure 5c).

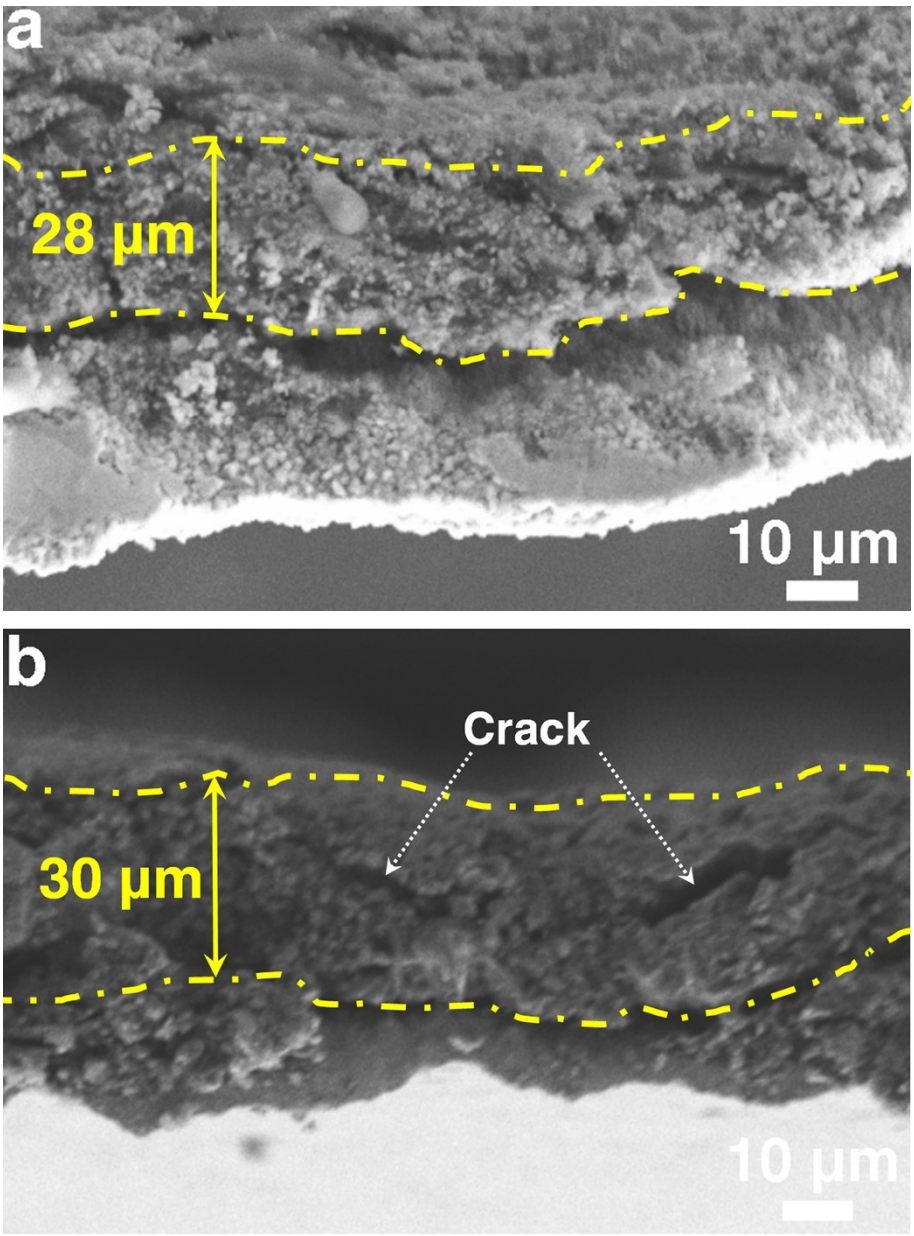

Figure S14. Cross-sectional view SEM images of the pristine electrodes of (a) $PbO_{1.44}$ NAHSs and (b) β-PbO_2 MSs.

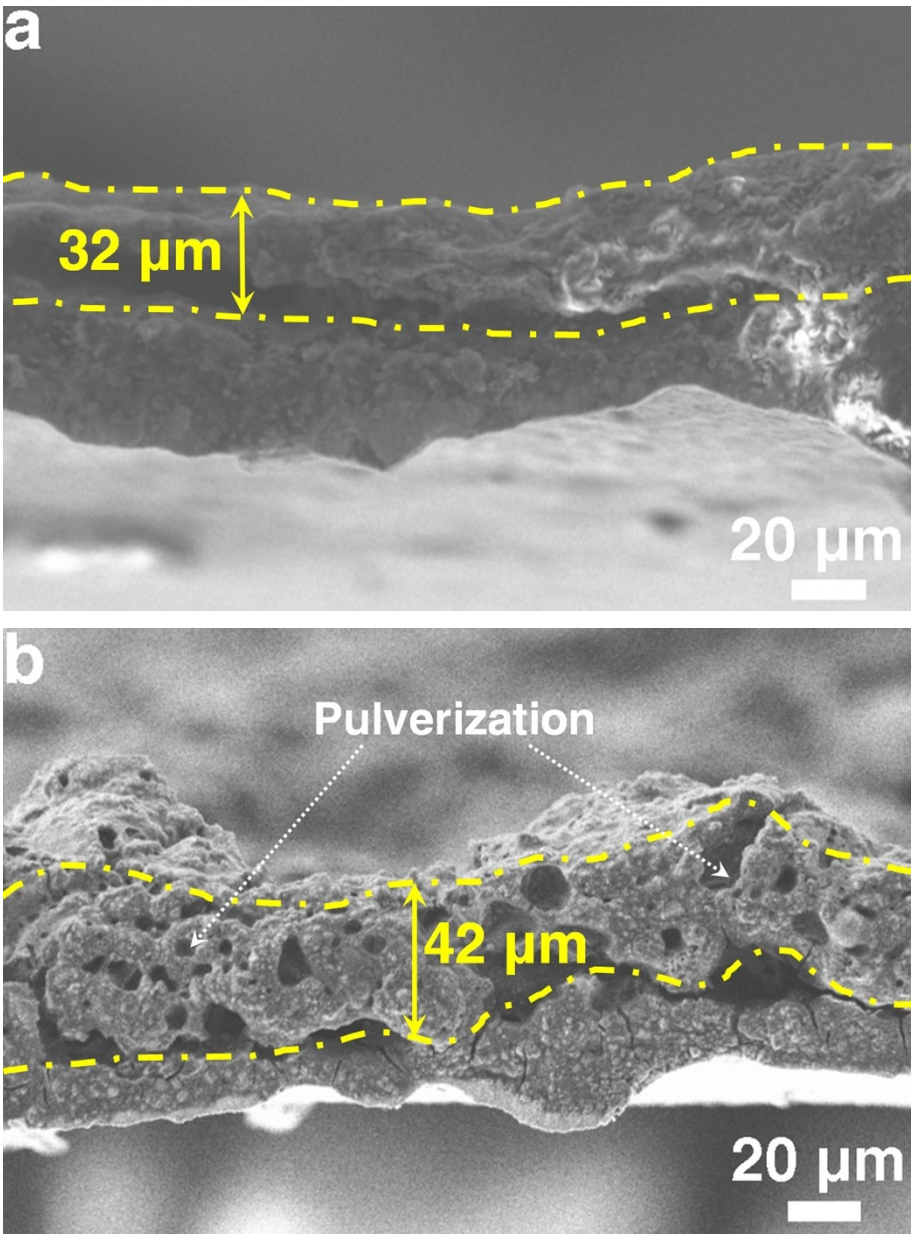

Figure S15. Cross-sectional view SEM images of the cycled electrodes of (a) β-PbO_2 MSs and (b) $PbO_{1.44}$ NAHSs obtained after the 90th cycle in the rate performance test (Figure 5c).

Table S1. Summary of the performances of $PbO_{1.44}$ NAHSs in our work and PbO_x-based materials in the literatures as anodes of LIBs. [1-10]

Sample	C-rate /mA g^{-1}	Cycle number	Capacity /mAh g^{-1}	Ref. No.	Sample No.
$PbO_{1.44}$ NAHSs	**50**	**100**	**561**	**This work**	
	500	**200**	**453**		
PbO film	0.25 mA cm^{-2}	40	500	1	[A]
PbO-C nanocomposites	0.1 mA cm^{-2}	50	100	2	[B]
Nanostructured PbO	0.1 mA cm^{-2}	50	60	3	[C]
PbO@C core-shell nanocomposites	0.3 mA cm^{-2}	50	170	4	[D]
PbO/Pb/C(B) nanocomposite	200	100	330	5	[E]
PbO-C nanocomposite	1000	100	250	6	[F]
Graphene oxide-coated PbO	50	200	240	7	[G]
$Pb_3Nb_4O_{13}$ nanowires	50	50	243	8	[H]
PbO powder	0.08 mA cm^{-2}	25	20	9	[I]
PbO nanoparticles	100	100	202.2	10	[J]

Notes: NAHSs: nanoparticle-assembled hollowspheres; C: carbon; C(B): boron doped carbon; Ref. No.: supplementary reference number; Sample No.: sample number in Figure 6l.

Supplementary References

1 M. Martos, J. Morales, R. A. L. Sa´nchez , D. Leinen, F. Martin and J. R. R. Barrado, *Electrochimi. Acta*, 2001, **46**, 2939−2948.

2 S. H. Ng, J. Wang, K. Konstantinov, D. Wexler, J. Chen and a. H. K. Liu, *J. Electrochem. Soc.*, 2006, **153**, A787−A793.

3 K. Konstantinov, S. H. Ng, J. Z. Wang, G. X. Wang, D. Wexler and H. K. Liu, *J. Power Sources*, 2006, **159**, 241−244.

4 Q. Pan, Z. Wang, J. Liu, G. Yin and M. Gu, *Electrochem. Commun.*, 2009, **11**, 917−920.

5 H. Wang, Y. Li, Y. Wang, J. Ma, S. Hu, H. Hou and J. Yang, *Ceram. Int.*, 2017, **43**, 12442−12451.

6 C.-H. Li, P. Sengodu, D.-Y. Wang, T.-R. Kuo and C.-C. Chen, *RSC Adv.*, 2015, **5**, 50245−50252.

7 A. Guo, E. Chen, B. R. Wygant, A. Heller and C. B. Mullins, *ACS Appl. Energy Mater.*, 2019, **2**, 3017−3020.

8 Z. Chen, X. Cheng, H. Yu, H. Zhu, R. Zheng, T. Liu, J. Zhang, M. Shui and J. Shu, *Ceram. Int.*, 2018, **44**, 17094−17101.

9 F. B. F. R. Lipparoni, S. Panero and B. Scrosati, *Ionics*, 2002, **8**, 177−182.

10 L. Zhan, X. Xiang, B. Xie and B. Gao, *Powder Technol.*, 2017, **308**, 30−36.